



Modified Sol-Gel Method of Synthesising a Mn⁴⁺-Doped Mg₂TiO₄: A Red Phosphor for Improved LED Performance

Bahaa Wathook^{1,2*}, Dhia A. Hassan¹

¹ Department of Chemistry, College of Education for Pure Sciences, University of Basrah, Basrah 61004, Iraq

² General Directorate of Basrah Education, Ministry of Education, Basrah 61001, Iraq

Corresponding Author Email: dhia.hassan@uobasrah.edu.iq

Copyright: ©2024 The authors. This article is published by IETA and is licensed under the CC BY 4.0 license (<http://creativecommons.org/licenses/by/4.0/>).

<https://doi.org/10.18280/acsm.480102>

ABSTRACT

Received: 6 September 2023

Revised: 10 October 2023

Accepted: 9 November 2023

Available online: 26 February 2024

Keywords:

LEDs, perovskite, photoluminescence, SEM, sol-gel, titanium (IV) isopropoxide, Mn⁴⁺

Mn⁴⁺-doped perovskite Mg₂TiO₄ holds significant promise for the advancement of LED-based white light sources, given its cost-effectiveness, abundance, and stability at elevated temperatures. In this study, we present a novel approach employing the sol-gel method for the synthesis of Mg₂TiO₄:Mn⁴⁺ phosphor. Notably, the gel solution underwent a controlled cooling process at 2°C for a complete day, resulting in reduced drying time, lower calcination temperature, shortened duration, and optimized concentrations of doped ions in the derived phosphors. We explore the influence of temperature and manganese ions on the crystal structure of the host material, and X-ray diffraction (XRD) analysis confirms the formation of a pure phase. Additionally, the X-ray energy dispersion spectroscopy (EDX) technique is employed to ascertain the compound's constituent proportions, revealing a crystallite size of 32.23 nm. The photoluminescence study demonstrates an emission spectrum at 480 nm in the red region. Integrating our prepared red phosphor with a commercial yellow phosphor YAG:Ce³⁺, the resulting LED, utilizing a 450 nm blue chip InGaN, exhibits a correlated color temperature (CCT) of 4607 K, presenting a cool white color with chromaticity coordinates of $x = 0.3594$ and $y = 0.3753$. The modified sol-gel method thus offers a promising avenue for the efficient synthesis of Mn⁴⁺-doped Mg₂TiO₄ red phosphors, enhancing LED performance.

1. INTRODUCTION

The progression of Light Emitting Diode (LED) technology has experienced significant advancements in recent decades. The widespread adoption of solid-state lighting, driven by bright and visible LEDs, attributes its success to their high efficiency, reliability, robust structure, low power consumption, and prolonged durability [1-4]. Presently, the prevalent method for generating white LEDs involves combining yellow phosphor material with blue LED chip light. In this approach, phosphor-converted particles absorb short-wavelength light emitted by the LED chip, transforming a portion of it into long-wavelength light [5]. Over the last decade, fluoride and Mn⁴⁺-activated oxide materials have garnered attention for their application in white LEDs, offering cost-effective alternatives to rare-earth-doped red phosphors [6, 7]. Combining yttrium garnet yellow phosphor with red phosphor excited by (Ga, In) N blue LEDs enhances the temperature and color rendering index of white LEDs. Mn⁴⁺-doped phosphors exhibit narrow red emission and broad ultraviolet-blue excitation, aligning with the ideal characteristics for red-emitting phosphors in blue-chip stimulated white LEDs. Creating an effective Mn⁴⁺-doped red-emitting phosphor requires careful consideration of Mn⁴⁺ precursor components and host materials. Mn⁴⁺ ions are sensitive to their environment, readily oxidizing to Mn⁷⁺ or

reducing to Mn²⁺. Furthermore, manganese exists in a stable MnO₂ form, challenging its regulation when in the free Mn⁴⁺ form. Common hosts include oxide and fluoride complexes with Ge⁴⁺, Ti⁴⁺, and Al³⁺ located in the center of octahedral sites. Oxide ions offer lower polarizability and higher covalence than fluoride ions, influencing the physicochemical features of the synthesis process [8-10].

LED lighting has revolutionized the industry due to its exceptional efficiency and cost-effectiveness [11]. The activated ions used for doping the solid host lattice significantly influence the fluorescence characteristics of the host. Mn⁴⁺, with three electrons in the empty 3d shell, emerges as a crucial transition element for fabricating phosphor compounds for LED applications. The cost-effectiveness of Mn⁴⁺ doped phosphor manufacturing techniques and the widespread availability of manganese ores contribute to their scientific appeal. The Mn⁴⁺ ion, with its active positive charge, is susceptible to substantial crystallographic field effects [12-14]. Emission spectra play a pivotal role in distinguishing between strong and weak crystalline field states [15, 16].

In recent years, perovskite has emerged as a promising optoelectronic material, particularly metal perovskite halides, owing to their photoluminescence yield, tunable bandgap, and enhanced color purity [17, 18]. Perovskite lamps (PeLEDs) are anticipated to rival organic LEDs (OLEDs) and inorganic LEDs (ILEDs) in the future, given their extended lifespan,

material availability, cost-effectiveness, manufacturing efficiency, and improved performance [19-23].

This study focuses on the production of red $\text{Mg}_2\text{TiO}_4:\text{Mn}^{4+}$ phosphor using the sol-gel technique with gel cooling at 2°C . The cooling process enhances polymerization conditions, leading to the formation of nanophosphors. The sol-solution cooling technique is employed to improve phosphor preparation conditions, reducing calcination and polymerization temperatures, and shortening calcination duration. Titanium (IV) isopropoxide is investigated as the titanium source. Additionally, the study explores the impact of varying calcination temperatures and Mn^{4+} ion concentrations on the photoluminescence properties of phosphors. The conditions for optimal performance and electronic transitions of the compound are determined. Finally, an LED incorporating $\text{Mg}_2\text{TiO}_4:\text{Mn}^{4+}$ phosphor is fabricated, and its electroluminescence and white light efficiency are thoroughly investigated.

2. EXPERIMENTAL

2.1 Preparation method

Magnesium titanium oxide phosphors powders $\text{Mg}_2\text{TiO}_4:\text{Mn}^{4+}$ were prepared separately at different

temperatures using the sol-gel method. By adding 2.34 mL of titanium (IV) isopropoxide drop by drop to 8.92 mL of ethylene glycol with continuous stirring for 30 min. Added 7.6848 g of citric acid with continuous stirring for one hour until completely dissolved. Added 0.004 g of manganese nitrate, stirring continuously for 30 min, and finally added 4.1026 g of magnesium chloride hexahydrate with continuous stirring for 30 min. The sol-solution was left in refrigeration at 2°C for one day. The gel was dried using a drying oven at a temperature of 130°C for 2 h, and placed in the oven at 350°C for 30 min. Left the charred polymer to cool, grind it with a mortar of garnet to turn it into black powder.. Finally, this powder is heated in the muffle furnace for two hours at 600°C . Left inside the furnace to cool gradually. We repeated the above steps for different solutions separately and heating at various temperatures ($650, 700, 750, 800, 850^\circ\text{C}$, respectively). For the purpose of studying the effect of manganese concentration Mn^{4+} on the host Mg_2TiO_4 , we repeat the above steps for separate solutions with different weights of manganese nitrate (0.002, 0.004, 0.006, 0.008, 0.01) g, respectively. Calcination temperature of 700°C for two hours to obtain a pure phase similar to the standard card PDF#00-025-1157. The Figure 1 shows the procedure of $\text{Mg}_2\text{TiO}_4:\text{Mn}^{4+}$ phosphor preparation.

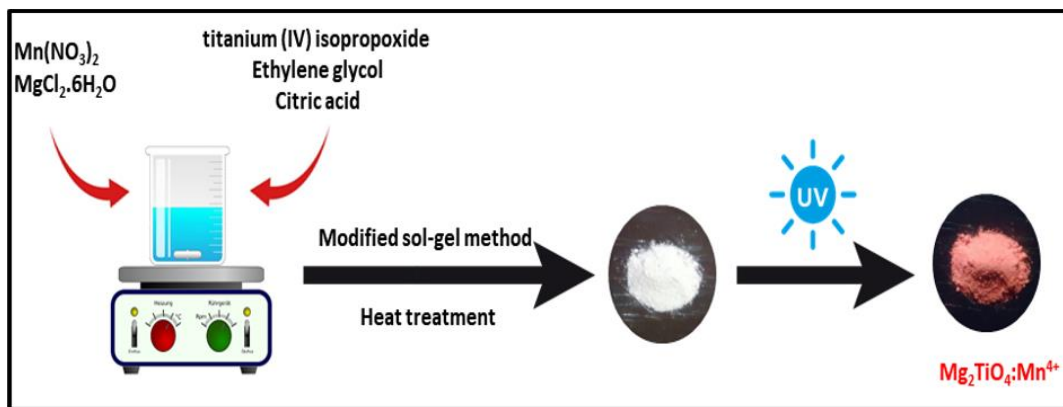


Figure 1. Schematic illustration of synthesis procedure of the $\text{Mg}_2\text{TiO}_4:\text{Mn}^{4+}$ compound

2.2 Characterizations

The synthesised compounds were detected using the XRD (Model X' Pert Pro Panalytical Company) at the 2θ (10° - 80°) range, where $\text{CuK}\alpha$ was used as the radiation source, at the 40 Kv voltage and 40 mA current. A fluorescence spectrophotometer was used to measure FT-IR. On the other hand, the particles were investigated using photoluminescence (PL) spectra with the CARY ECLIPSE-Varian Co. that was equipped with the 450-watt xenon lamp as an excitation source. Furthermore, energy dispersive X-ray spectroscopy (EDS) analysis was also conducted. The morphology of all synthesised particles was investigated with the Scanning Electron Microscope (SEM) and FESEM (Zeiss Model SIGMA VP), which were equipped with EDS. The researchers also determined the quantum efficiency using an Edinburg FLS10003 at the excitation wavelength of 467 nm.

3. RESULTS AND DISCUSSION

The influence of temperature on $\text{Mg}_2\text{Ti}_{(1-x)}\text{O}_4:\text{xMn}^{4+}$ phase

formation that was synthesised by the sol-gel method was assessed for 2 h at various temperatures ($600, 650, 700, 750, 800, 850^\circ\text{C}$) for all models. Figure 2 shows the XRD spectra of the generated compound. The XRD patterns for the phosphor mixtures show intense peaks induced by the reflections of cubic Mg_2TiO_4 , which were crystallised properly with the sol-gel method [24, 25]. The results indicated that a temperature value of 700°C was optimal for manufacturing the compound and generating the pure phase wherein the XRD peaks match the standard card (PDF #00-025-1157) [26], which reflects the purity of the compound. Wide spectral bands were noted at 600°C , implying that the compound was amorphous. However, at 650°C , wide XRD peaks were noted that did not agree with the standard card PDF #00-025-1157, indicating an impure phase. On the other hand, the peaks were observed at 2θ ($24.07, 21.23$) at other temperature values ($750, 800, 850^\circ\text{C}$). The synthesis of the MgTiO_3 phase, which corresponds to the standard card PDF #00-006-494, is attributed to Mg_2TiO_4 disintegration at higher temperatures. The XRD spectrum of the red phosphor is shown in Figure 3, and the displayed peaks suggest that the

sol-gel process could effectively crystallise the powders. These peaks validate the crystalline nature of compound along with its pure state, and all the peaks comply with the standard cards (PDF #00-025-1157), with the following Unit Cell Parameters: Cell Volume = 601.40 Å, $a = 8.4409$ Å, $b = 8.4409$ Å, $c = 8.4409$ Å, and the space group of Fd-3m [23-27], indicating that the synthesised compound was properly synthesised in a pure phase [28-31]. The results also revealed that none of the established samples exhibited any impure phase [32-34]. Furthermore, no change was detected in the host's XRD spectrum after the addition of Mn^{4+} ions, indicating that the doped ions were linked to the crystal Mg_2TiO_4 lattice [35-37]. The peak diffraction of the $Mg_2TiO_4:Mn^{4+}$ samples was seen to turn slightly to a high angle, as Mn^{4+} showed a smaller radius than Ti^{4+} .

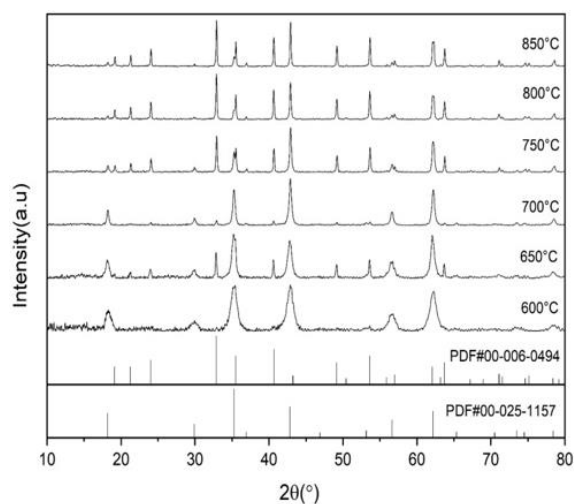


Figure 2. XRD of $Mg_2TiO_4:Mn^{4+}$ at different temperatures

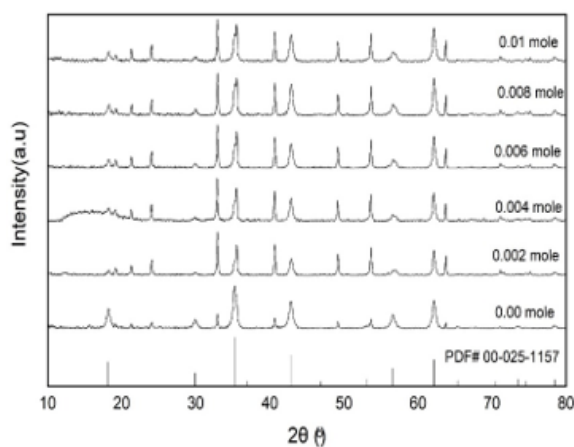


Figure 3. The XRD patterns of $Mg_2TiO_4:Mn^{4+}$ compound at different Mn^{4+} concentrations

Figure 4 shows SEM images of the $Mg_2TiO_4:Mn^{4+}$ compound that was synthesised using the sol-gel method at various temperatures (600, 650, 700, 750, 800, and 850°C) for 2 h. The SEM images were compared to the XRD values at 700°C and verified the fabrication of the pure phase. The images demonstrate the formation of a nano-compound with spherical particles having a smooth surface. Any modification in the shape of the phosphors can significantly affect the photoluminescence intensity of the synthesised materials. The crystallite size was computed with Scherrer's equation and was found to be 32.23 nm at an $Mg_2TiO_4:Mn^{4+}$ concentration of

0.002 mol, with a six-faceted crystal structure. Figure 5 show the compound's crystal structure. The infiltration of any impurity into the crystal structure does not alter its structure, particularly when the doped ion displays a radius similar to that of the replaced ion. Also, when the Mn^{4+} ion enters the host Mg_2TiO_4 composition, it replaces a minor quantity of Ti^{4+} ions.

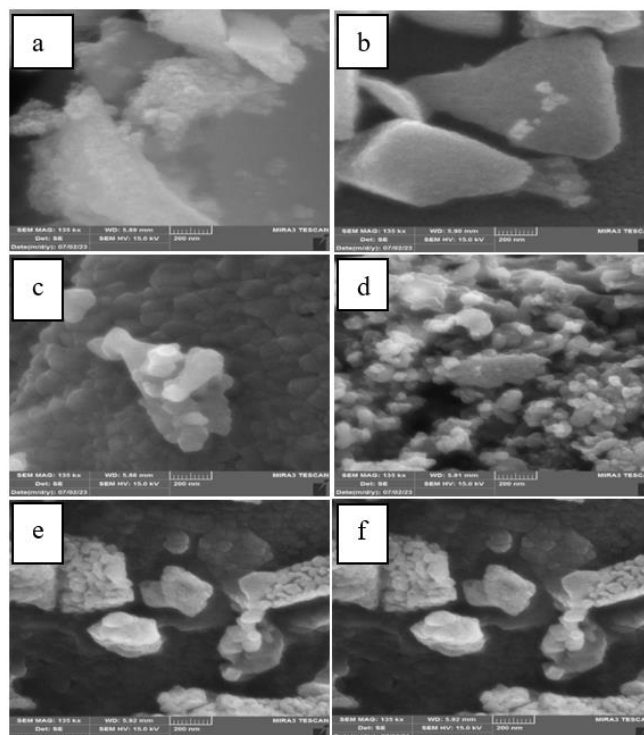


Figure 4. The SEM images of the $Mg_2TiO_4:Mn^{4+}$ compound at (a) 600°C, (b) 650°C, (c) 700°C, (d) 750°C, (e) 800°C, and (f) 850°C

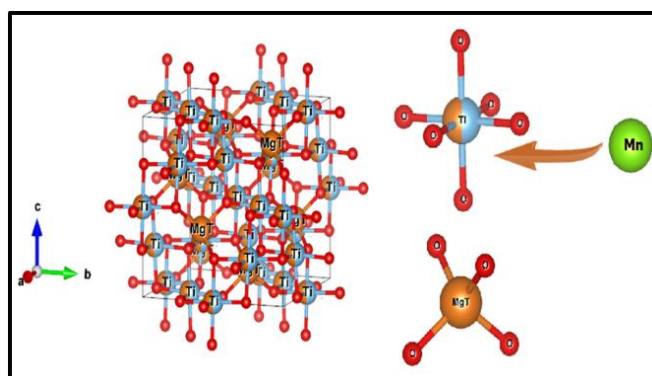


Figure 5. The crystal structure of the $Mg_2TiO_4:Mn^{4+}$ compound

The concentration quenching phenomenon causes a decrease in fluorescence and PL intensity as the Mn^{4+} ion concentration is increased. The Ti-O bond present in the $Mg_2TiO_4:Mn^{4+}$ phosphor was stronger compared to the Mn-O bond because of the large Ti^{4+} ionic radius, wherein every Ti^{4+} ion was surrounded by six O^{2-} ions and Mg^{2+} ion was surrounded by four O^{2-} ions to yield a uniform polyhedron. The doped Mn^{4+} ions penetrate the host Mg_2TiO_4 compound structure, and a partial replacement of Ti^{4+} ions generate MnO_2 with a cubic shape [38, 39]. Figure 6 shows FTIR of $Mg_2TiO_4:Mn^{4+}$, the absorption bands at (462.92, 478.35) cm^{-1}

are ascribed to bending vibrations and asymmetric stretching vibrations of the Mg-O bond [40], whereas the band at 570.93 cm^{-1} corresponds to Ti-O bond stretching vibrations [41]. Furthermore, the band at 1743.66 cm^{-1} could be attributed to the Mg-O-Ti bond stretching vibrations. Figure 7 shows the photoluminescence emission spectra (PL) of $\text{Mg}_2\text{Ti}_{(1-x)}\text{O}_4:\text{xMn}^{4+}$. Where $x = 0.002, 0.004, 0.006, 0.008, 0.01$ mole, at the excitation wavelength of 480 nm, varying Mn^{4+} concentrations, and a 700 °C temperature. The results in the figure demonstrate the presence of a wide emission beam between (580-780 nm) because of the forbidden transition of $d \rightarrow d$ of ${}^2\text{E}_g \rightarrow {}^4\text{A}_2g$. This could be attributed to the concentration of the Mn^{4+} ions at 657 nm.

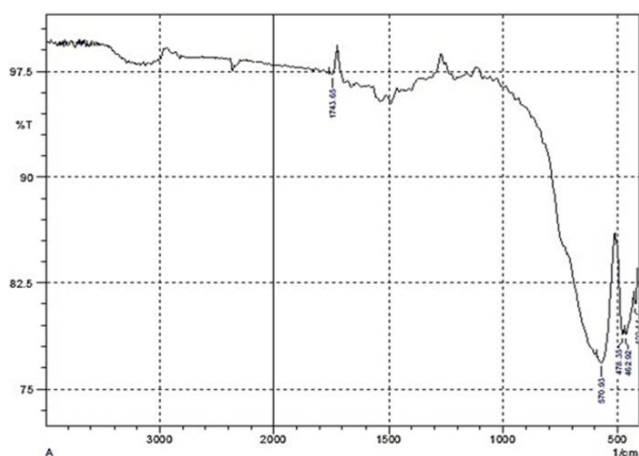


Figure 6. The infrared spectrum (FTIR) of $\text{Mg}_2\text{TiO}_4:\text{Mn}^{4+}$

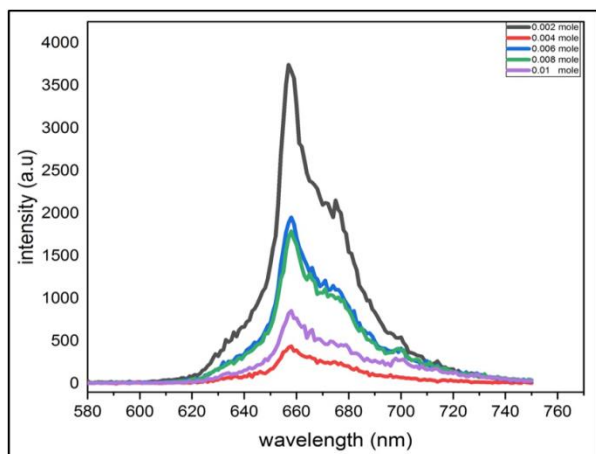


Figure 7. The photoluminescence emission spectra (PL) of $\text{Mg}_2\text{Ti}_{(1-x)}\text{O}_4:\text{xMn}^{4+}$

Figure 8a shows SEM images of the Mg_2TiO_4 compound that was doped with Mn^{4+} ions at a 0.002 mol concentration and a calcination temperature of 700°C for 2 h. These results indicate that these nano-sized crystals show a hexagonal geometrical shape with a smooth polished surface. Figure 8b shows the EDS spectra of $\text{Mg}_2\text{TiO}_4:\text{Mn}^{4+}$. The presence of elemental components like Mg, Ti, O, and Mn in the sample was confirmed by EDS, with atomic percentages of these elements being 29.38%, 20.25%, 50.08%, and 0.29%, respectively. The percentages of all elements were confirmed by their appearance in EDS spectra. Figure 8c shows the mapping of the $\text{Mg}_2\text{TiO}_4:\text{Mn}^{4+}$ compound and every component based on their distinct colour. Figure 9a shows the luminescence of $\text{Mg}_2\text{TiO}_4:\text{Mn}^{4+}$ phosphors at a 0.02 g

concentration of Mn^{4+} ions before and after UV lamp irradiation at a wavelength of 365 nm. Figure 9b shows the electroluminescence spectra of LED lamps, which showed two emission peaks. The first can be attributed to the electroluminescence of blue chips at 449 nm, the second could be attributed to yellow YAG phosphor at 566 nm, while the remaining red hue was ascribed to the $\text{Mg}_2\text{TiO}_4:\text{Mn}^{4+}$ compound at 585 nm. The synthesised compound is effective and shows a higher colour rendering quality when utilised in LED applications with a CRI of 69.7. Figure 9c shows the correlated colour temperature (CCT) coordinates of the synthesised compound at 4607 K and chromaticity coordinates of Commission Internationale de L'éclairage (CIE), i.e., $X = 0.3594$ and $Y = 0.3753$.

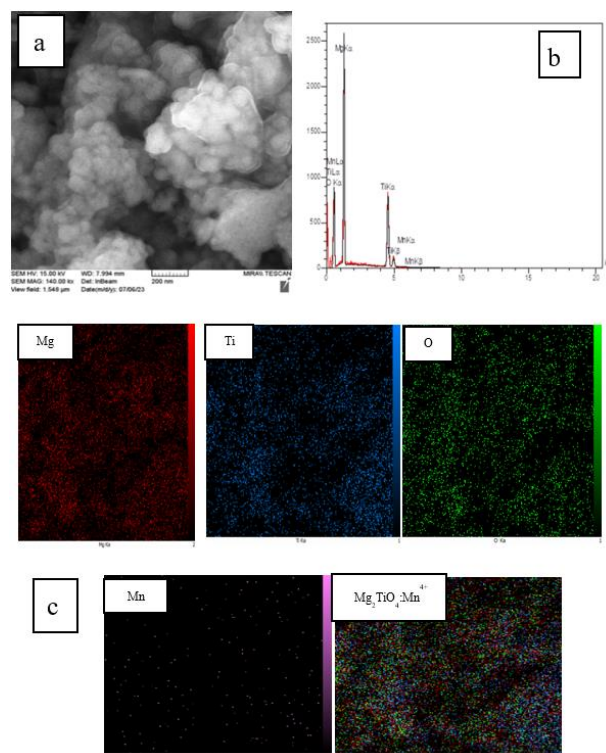


Figure 8. a. SEM; b. EDS spectrum c. EDS mapping; of the $\text{Mg}_2\text{TiO}_4:\text{Mn}^{4+}$ particles

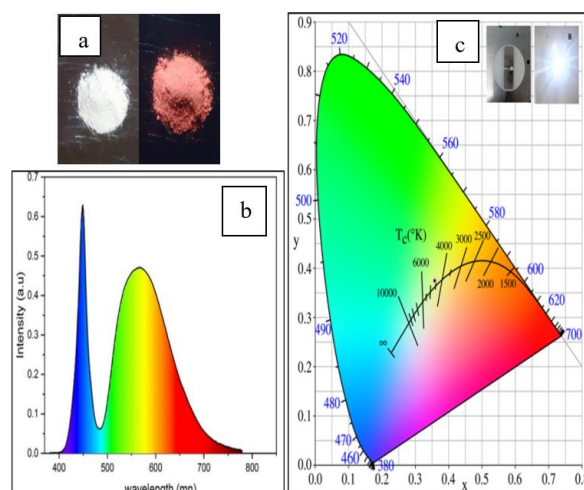


Figure 9. a. The luminescence of $\text{Mg}_2\text{TiO}_4:\text{Mn}^{4+}$ pre- and post-exposure to 365 nm-wavelength UV irradiation; b. the electroluminescence spectra of the LED lamps; c. their CIE color diagram

4. CONCLUSION

The cooling agent affected the production of the $Mg_2Ti_{(1-x)}O_4 \cdot xMn^{4+}$ phosphor using the sol-gel method since the heat was not used to fabricate the gel solution, and the activator concentration was comparatively low in comparison to the other methods. We also employed an experimental approach for acquiring the best optical properties of a cool white LED. The phosphor compound displays the CCT coordinates of the manufactured compound at 4607 K and CIE chromaticity coordinates of $X = 0.3594$ and $Y = 0.3753$. The results further showed that a concentration of 0.002 moles displayed a specific optical effect since this compound showed high morphology and high fluorescence at the excitation wavelength of 480 nm. It was discovered that with an increase in the Mn^{4+} ion concentration, the fluorescence of the produced phosphors was reduced owing to the luminescence quenching phenomenon. As a result, this method could be used in many applications like manufacturing display screens, low-cost lights, and semiconductor materials.

ACKNOWLEDGMENTS

This work is supported by Chemistry Department, College of Education for Pure Sciences, University of Basrah, Iraq, as part of the master research graduation requirements.

REFERENCES

[1] Pattison, M., Hansen, M., Bardsley, J., Thomson, G., Gordon, K., Walkerson, A., Lee, K., Nubbe, V., Donnelly, S. (2022). Solid-State Lighting R&D Opportunities. Guidehouse, Washington, DC, United States. <https://doi.org/10.13140/RG.2.2.16101.47844>

[2] Phillips, J.M., Coltrin, M.E., Crawford, M.H., Fischer, A.J., Krames, M.R., Mueller-Mach, R., Mueller, G.O., Ohno, Y., Rohwer, L.E.S., Simmons, J.A., Tsao, J.Y. (2007). Research challenges to ultra-efficient inorganic solid-state lighting. *Laser & Photonics Reviews*, 1(4): 307-333. <https://doi.org/10.1002/lpor.200710019>

[3] Xie, R.J., Li, Y.Q., Hirosaki, N., Yamamoto, H. (2016). Nitride Phosphors and Solid-State Lighting (1st ed.). CRC Press.

[4] Sun, Y., Jiang, Y., Sun, X.W., Zhang, S., Chen, S. (2019). Beyond OLED: Efficient quantum dot light-emitting diodes for display and lighting application. *The Chemical Record*, 19(8): 1729-1752. <https://doi.org/10.1002/tcr.201800191>

[5] Luo, X., Hu, R. (2014). Calculation of the phosphor heat generation in phosphor-converted light-emitting diodes. *International Journal of Heat and Mass Transfer*, 75: 213-217. <https://doi.org/10.1016/j.ijheatmasstransfer.2014.03.067>

[6] Li, J., Yan, J., Wen, D., Khan, W.U., Shi, J., Wu, M., Tanner, P.A. (2016). Advanced red phosphors for white light-emitting diodes. *Journal of Materials Chemistry C*, 4(37): 8611-8623. <https://doi.org/10.1039/C6TC02695H>

[7] Hong, F., Xu, H., Yang, L., Liu, G., Song, C., Dong, X., Yu, W. (2019). Mn^{4+} nonequivalent-doped Al^{3+} -based cryolite high-performance warm WLED red phosphors. *New Journal of Chemistry*, 43(37): 14859-14871. <https://doi.org/10.1039/C9NJ03607E>

[8] Kawakita, S., Kominami, H., Hara, R. (2015). Preparation and photoluminescence properties of Mn doped deep red emitting phosphor under blue to near ultraviolet excitations. *Physica Status Solidi (c)*, 12(6): 805-808. <https://doi.org/10.1002/pssc.201400323>

[9] Xu, J., Hassan, D.A., Zeng, R., Peng, D. (2015). Sr₁₋₉₈Eu_{0.02}SiO₄ luminescence whisker based on vapor-phase deposition: Facile synthesis, uniform morphology and enhanced luminescence properties. *Materials Research Bulletin*, 71: 106-110. <https://doi.org/10.1016/j.materresbull.2015.07.007>

[10] Xu, J., Hassan, D.A., Zeng, R.J., Peng, D.L. (2016). Lu₃Al₅O₁₂: Ce@ SiO₂ phosphor-in-glass: its facile synthesis, reduced thermal/chemical degradation and application in high-power white LEDs. *Journal of the European Ceramic Society*, 36(8): 2017-2025. <https://doi.org/10.1016/j.jeurceramsoc.2016.01.007>

[11] He, S., Xu, F., Han, T., Lu, Z., Wang, W., Peng, J., Ye, X. (2020). A Mn⁴⁺-doped oxyfluoride phosphor with remarkable negative thermal quenching and high color stability for warm WLEDs. *Chemical Engineering Journal*, 392: 123657. <https://doi.org/10.1016/j.cej.2019.123657>

[12] Zhou, Q., Dolgov, L., Srivastava, A.M., Zhou, L., Wang, Z., Shi, J., Wu, M. (2018). Mn²⁺ and Mn⁴⁺ red phosphors: Synthesis, luminescence and applications in WLEDs: A review. *Journal of Materials Chemistry C*, 6(11): 2652-2671. <https://doi.org/10.1039/C8TC00251G>

[13] Li, Y., Qi, S., Li, P., Wang, Z. (2017). Research progress of Mn doped phosphors. *RSC advances*, 7(61): 38318-38334. <https://doi.org/10.1039/C7RA06026B>

[14] Medić, M.M., Brik, M.G., Dražić, G., Antic, Z.M., Lojpur, V.M., Dramićanin, M.D. (2015). Deep-red emitting Mn⁴⁺ doped Mg₂TiO₄ nanoparticles. *The Journal of Physical Chemistry C*, 119(1): 724-730. <https://doi.org/10.1021/jp5095646>

[15] Hassan, D.A., Xu, J., Zeng, R. (2016). Role of synthesis method and α , β -Sr (2-x) SiO₄: xEu²⁺ phases on the photoluminescent properties of Sr (1-x) Si₂O₂N₂: xEu²⁺ phosphors. *Materials Research Bulletin*, 83: 468-473. <https://doi.org/10.1016/j.materresbull.2016.06.024>

[16] Mueller-Mach, R., Mueller, G.O., Krames, M.R., Trottier, T. (2002). High-power phosphor-converted light-emitting diodes based on III-nitrides. *IEEE Journal of Selected Topics in Quantum Electronics*, 8(2): 339-345. <https://doi.org/10.1109/2944.99918917>

[17] Lee, H., Park, J., Kim, S., Lee, S.C., Kim, Y.H., Lee, T.W. (2020). Perovskite emitters as a platform material for down-conversion applications. *Advanced Materials Technologies*, 5(10): 2000091. <https://doi.org/10.1002/admt.202000091>

[18] Khirade, P.P., Raut, A.V. (2022). Perovskite Structured Materials: Synthesis, Structure, Physical Properties and Applications. In *Recent Advances in Multifunctional Perovskite Materials*. IntechOpen. <https://doi.org/10.5772/intechopen.106252>

[19] Cho, H., Kim, Y.H., Wolf, C., Lee, H.D., Lee, T.W. (2018). Improving the stability of metal halide perovskite materials and light-emitting diodes. *Advanced Materials*, 30(42): 1704587. <https://doi.org/10.1002/adma.201704587>

[20] Tiwari, A., Satpute, N.S., Mehare, C.M., Dhoble, S.J. (2021). Challenges, recent advances and improvements for enhancing the efficiencies of ABX₃-based PeLEDs

- (perovskites light emitting diodes): A review. *Journal of Alloys and Compounds*, 850: 156827. <https://doi.org/10.1016/j.jallcom.2020.156827>
- [21] Wei, Y., Cheng, Z., Lin, J. (2019). An overview on enhancing the stability of lead halide perovskite quantum dots and their applications in phosphor-converted LEDs. *Chemical Society Reviews*, 48(1): 310-350. <https://doi.org/10.1039/C8CS00740C>
- [22] Shi, Q., Hassan, D.A., Zeng, R. (2014). Photoluminescence properties of Na_{1.45}La_{8.55}(SiO₄)₆(F_{0.9}O_{1.1}):Eu for applications as a reddish orange phosphor. *Functional Materials Letters*, 7(5): 1450060. <https://doi.org/10.1142/S179360471450060X>
- [23] Shinde, K.N., Dhoble, S.J., Swart, H.C., Park, K., Shinde, K.N., Dhoble, S.J., Park, K. (2012). Basic mechanisms of photoluminescence. *Phosphate Phosphors for Solid-State Lighting*, 41-59. <https://doi.org/10.1007/978-3-642-34312-4>
- [24] Choi, J. I. (2014). Electrophoretic Deposition of Highly Efficient Phosphors for White Solid State Lighting using near UV-Emitting LEDs. University of California, San Diego.
- [25] Ye, T., Li, S., Wu, X., Xu, M., Wei, X., Wang, K., Chen, J. (2013). Sol-gel preparation of efficient red phosphor Mg₂TiO₄:Mn⁴⁺ and XAFS investigation on the substitution of Mn⁴⁺ for Ti⁴⁺. *Journal of Materials Chemistry C*, 1(28): 4327-4333. <https://doi.org/10.1039/C3TC30553H>
- [26] Mandal, S. (2022). Investigation of Zinc Aluminate as a Refractory Material (Doctoral dissertation, The University of Alabama at Birmingham).
- [27] Llusar, M., García, E., García, M.T., Gargori, C., Badenes, J.A., Monrós, G. (2015). Stability and coloring properties of Ni-qandilite green spinels (Ni, Mg)₂TiO₄: The “half color wheel” of Ni-doped magnesium titanates. *Dyes and Pigments*, 122: 368-381. <https://doi.org/10.1016/j.dyepig.2015.07.014>
- [28] Liu, L., Meng, Z., Wang, X., Chen, H., Duan, Z., Zhou, X., Liu, Z. (2023). Semiconducting transport in Pb_{10-x}Cu_x(PO₄)₆O sintered from Pb₂So₅ and Cu₃P. *Advanced Functional Materials*, 2308938. <https://doi.org/10.1002/adfm.202308938>
- [29] Bojdys, M.J., Müller, J.O., Antonietti, M., Thomas, A. (2008). Ionothermal synthesis of crystalline, condensed, graphitic carbon nitride. *Chemistry—A European Journal*, 14(27): 8177-8182. <https://doi.org/10.1002/chem.200800190>
- [30] Lu, C., Wang, J., Cao, D., Guo, F., Hao, X., Li, D., Shi, W. (2023). Synthesis of magnetically recyclable g-C₃N₄/NiFe₂O₄ S-scheme heterojunction photocatalyst with promoted visible-light-response photo-Fenton degradation of tetracycline. *Materials Research Bulletin*, 158: 112064. <https://doi.org/10.1016/j.materresbull.2022.112064>
- [31] Wang, K., Yan, T., Zhao, Y.M., Li, G.D., Pan, W.G. (2022). Preparation and thermal properties of palmitic acid@ ZnO/Expanded graphite composite phase change material for heat storage. *Energy*, 242: 122972. <https://doi.org/10.1016/j.energy.2021.122972>
- [32] Bulger, P.G., Conlon, D.A., Cink, R.D., Fernandez-Cerezo, L., Zhang, Q., Thirumalairajan, S., Chalgeri, A. (2023). Drug-linkers in antibody-drug conjugates: Perspective on current industry Practices. *Organic Process Research & Development*, 27(7): 1248-1257. <https://doi.org/10.1021/acs.oprd.3c00136>
- [33] Sun, L., Berndt, C.C., Gross, K.A., Kucuk, A. (2001). Material fundamentals and clinical performance of plasma-sprayed hydroxyapatite coatings: A review. *Journal of Biomedical Materials Research: An Official Journal of The Society for Biomaterials, The Japanese Society for Biomaterials, and The Australian Society for Biomaterials and the Korean Society for Biomaterials*, 58(5): 570-592. <https://doi.org/10.1002/jbm.1056>
- [34] Chung, S.Y., Bloking, J.T., Chiang, Y.M. (2002). Electronically conductive phospho-olivines as lithium storage electrodes. *Nature Materials*, 1(2): 123-128. <https://doi.org/10.1038/nmat732>
- [35] Sun, D., Li, P., Zhang, J., Zhang, J., Xue, Y., Shi, H. (2015). The effect of Li⁺ on structures and luminescence properties of ZnAl₂O₄:Mn²⁺ (Mn⁴⁺), Li⁺ phosphors. *Dalton Transactions*, 44: 7854-7861. <https://doi.org/10.1039/C4DT03967J>
- [36] Han, M., Liu, L., Zhang, D., Du, Y., Zhao, L., Wang, Y., Lv, L. (2022). Tuning the morphology of Mg₂TiO₄:Mn⁴⁺ for luminescence performance and latent fingerprint visualization. *Journal of Luminescence*, 252: 119417. <https://doi.org/10.1016/j.jlumin.2022.119417>
- [37] Chang, S., Hu, Y., Qian, J., Shao, Y., Ni, S., Kong, L., Dan, W., Luo, C., Jin, S., Xu, X. (2021). Mg₂TiO₄ spinel modified by nitrogen doping as a Visible-Light-Active photocatalyst for antibacterial activity. *Chemical Engineering Journal*, 410: 128410. <https://doi.org/10.1016/j.cej.2021.128410>
- [38] Song, Z., Zhao, J., Liu, Q. (2019). Luminescent perovskites: recent advances in theory and experiments. *Inorganic Chemistry Frontiers*, 6(11): 2969-3011. <https://doi.org/10.1039/C9QI00777F>
- [39] Hu, R., Luo, X., Zheng, H., Qin, Z., Gan, Z., Wu, B., Liu, S. (2012). Design of a novel freeform lens for LED uniform illumination and conformal phosphor coating. *Optics Express*, 20(13): 13727-13737. <https://doi.org/10.1364/OE.20.013727>
- [40] Zahro, S., Ermawati, F.U. (2018). Analisis struktur dan komposisi fasa serbuk Mg₂TiO₄. *Inovasi Fisika Indonesia*, 7(2): 63-66. <https://doi.org/10.26740/ifi.v7n2.p%25p>
- [41] Han, M., Tang, H., Liu, L., Wang, Y., Zhang, X., Lv, L. (2021). Tuning the Mn⁴⁺ coordination environment in Mg₂TiO₄ through a codoping strategy for enhancing luminescence performance. *The Journal of Physical Chemistry C*, 125(28): 15687-15695. <https://doi.org/10.1021/acs.jpcc.1c04293>